Zeitschrift Kunststofftechnik
Journal of Plastics Technology

archival, peer-reviewed online Journal of the Scientific Alliance of Polymer Technology
archivierte, peer-rezensierte Internetzeitschrift des Wissenschaftlichen Arbeitskreises Kunststofftechnik (WAK)
www.plasticseng.com, www.kunststofftech.com

handed in/eingereicht: 08.12.2012
accepted/angenommen: 07.02.2012

Prof. Dr.-Ing. Christian Hopmann[1], Prof. Dr.-Ing. Dr.-Ing. E. h. Walter Michaeli[1], Stephan Eilbracht[1], Prof. Dr.-Ing. Kirsten Bobzin[2], Dr.-Ing. Nazlim Bagcivan[2], Sebastian Theiß[2], Claudia Hartmann[3], Dr.-Ing. Jens Holtkamp[3], Dr.-Ing. Arnold Gillner[3], Univ.-Prof. Dr. rer. nat. J. Mayer[4]

[1] Institut für Kunststoffverarbeitung, RWTH Aachen
[2] Institut für Oberflächentechnik, RWTH Aachen
[3] Fraunhofer Institut für Lasertechnik, RWTH Aachen
[4] Gemeinschaftslabor für Elektronenmikroskopie, RWTH Aachen

Extrusion embossing of hydrophobic films – a study on process characteristics and surface properties

The variothermal extrusion embossing process is capable of replicating micro structures on polymer film surfaces. After a summary of the entire process chain and the technology of variothermal extrusion embossing, this paper discusses in detail the fabrication of hydrophobic LD-PE films that are inspired by the lotus flower. The dependency of the obtained surface structure geometry and functionality on the process is analysed. Static contact angles for purified water up to 150° are achieved as well as aspect ratios up to 4 due to the formation of hair-like structures during demoulding.

Extrusionsprägen hydrophober Kunststoff-folien – eine Analyse von Prozessmerkmalen und Oberflächeneigenschaften

Das variotherme Extrusionsprägen ist geeignet, schnell und kostengünstig mikrostrukturierte Kunststofffolien herzustellen. Neben einer Darstellung der Prozesskette und der zugrunde liegenden Technologie liegt der Schwerpunkt dieser Veröffentlichung auf der Herstellung hydrophober LD-PE Folien nach dem Vorbild der Lotus-Blume. Die Abhängigkeit der Oberflächenstruktur und ihrer Funktionalität von der Prozessführung wird analysiert. Statische Kontaktwinkel bis 150° für deionisiertes Wasser werden erreicht. Durch die Bildung von Mikrohärchen während der Entformung werden Aspektverhältnisse bis 4 realisiert.

Extrusion embossing of hydrophobic films – a study on process characteristics and surface properties

Ch. Hopmann, W. Michaeli, S. Eilbracht, K. Bobzin, N. Bagcivan, S. Theiß, C. Hartmann, J. Holtkamp, A. Gillner, J. Mayer

1 INTRODUCTION

Studying nature's phenomena with respect to surface functionality, an enormous variety of exceptionally shaped surfaces with structures on micro- and nanoscale are found. In many cases the surface topology in combination with the surface chemistry of the material is responsible for striking effects and behaviour. Examples include the well-known shark-skin-effect where a rough, riblet-like surface structure reduces flow resistance [1]. Another example is the surface texture of gecko feet resulting in its extraordinary ability to climb even smooth vertical surfaces and seemingly defy gravity [2,3]. For optical applications the eye of a moth is often used as a biomimetic prototype for a non-reflective surface enabling ideal light injection [4]. Besides all these examples one of the most popular and widely studied natural surfaces is the one of the lotus leaf (Nelumbo nucifera) as described in detail by Barthlott et al. [5,6]. A bump-like surface structure in the micro- and nanoscale gives those leaves the ability to repel water. Water drops from rain or thaw cannot stick to the surface and roll off. This not only results in perfectly dry surfaces but also in perfectly clean surfaces as the water drops take dirt and dust particles with them. The effect is predominantly based upon the combination of surface structure and a surface material with low surface energy.

The variety of surface structures and the diversity of effects observed consequently lead to the idea of mimicking these surfaces for technical applications. Figure 1 gives a brief overview of the huge number of possible applications. In recent years the manufacturing of micro-structured parts became more and more applicable and slowly grew from laboratory scale to industrial production processes. Common examples are the manufacturing of CDs or DVDs, holograms for security features, shark-skin structured swim suits, retro reflective films or microfluidic devices and optical components to cite a few [7,8].

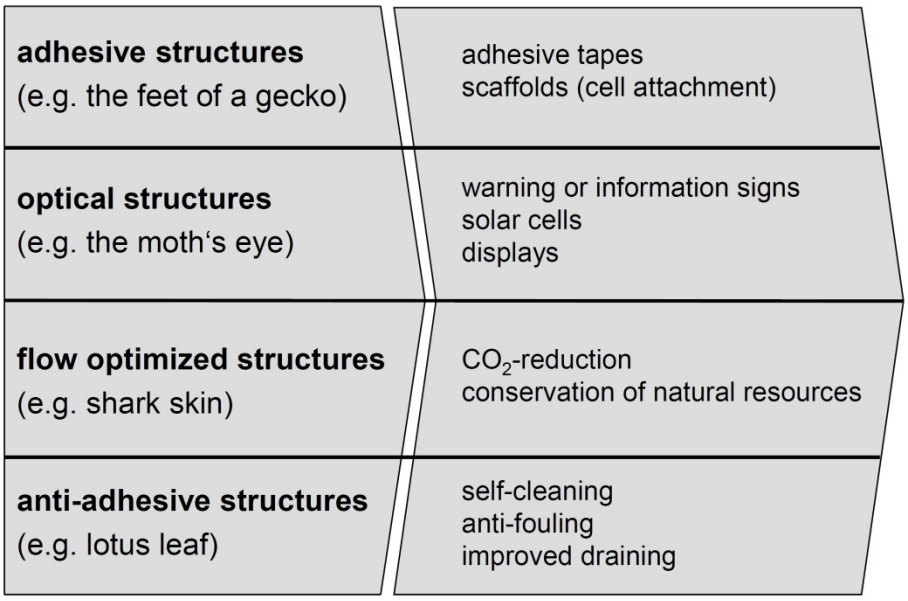

Figure 1: Prototype nature – transferring ideas to mass production products

Technologies for manufacturing of parts with micro- or nanoscaled surface features range from sol-gel techniques, solution casting and electrospinning and -spraying to silicon wet etching and deep reaction ion etching. Other methods include the application of nanotubes by chemical vapour deposition (CVD) for the modification of surfaces or lithographic methods (LIGA) using x-ray or UV radiation and electroplating for the fabrication of parts [7,9-13]. Furthermore, printing technologies like nanoimprinting (UV-based or thermal), microcontact printing (μCP) and direct writing methods using scanning probe microscopy or ink-jet printing are suitable to create well defined surface structures [14]. Other techniques include micro machining (drilling, milling, turning) and laser ablation as well as electric discharge machining for the manufacturing of samples that can even have complex three-dimensional shapes [7,9,15].

Many of these techniques work well in laboratory scale and are suited for the manufacturing of prototypes and small batches for research. Usually the costs and/or the limitations concerning processable materials, part geometries as well as the time-consuming manufacturing processes themself limit the application of many of these techniques for industrial purposes. However, they are well suited for fabrication of tools with master surfaces that can be used for replication in a following production step. Having a mass production market in mind replication techniques are likely the solution of choice [7]. Especially when polymeric materials are to be structured, a master containing the negative surface topology is designed with one of the aforementioned methods. This master is then used for replication. Depending on the structure of the surface (aspect ratio, shape of edges, tolerances), the size and shape of the final part and the batch size strived for, the reproduction method is chosen. Injection moulding or reactive injection moulding [7] is chosen for large numbers of parts with limited dimensions and three-dimensional shape, hot embossing for flat

parts of high quality and high aspect ratios (often optical parts) [16,17]. Other possible reproduction methods for mass-production purposes mentioned in literature are roller embossing [18,19] and extrusion embossing [20,21,22,23] (both methods are related to hot embossing) as well as thermoforming [7].

Roller embossing (thermal or UV-based) enables the continuous production of polymeric films and plates by exchanging the discontinuously working stamp of the hot embossing process by an embossing roll. However, this changes the process, for example the time for the replication is now limited and depending on the rotation speed and diameter of the embossing roll. Also pressure (responsible for the filling of the structures and for the avoidance of shrinkage) is not applied during cooling. Furthermore, the replication of deep structures is still challenging [19]. Another process-related difference is the direction of demoulding. For roller embossing a peeling motion has to be considered in contrast to a movement perpendicular to the mould's surface for hot embossing. The big advantages of roller embossing compared to hot embossing are the achievable production rates (60 m/min by 2 m width are reported [19]). Although numerous attempts have been made to reduce the cycle times in hot embossing (e.g. variothermal approaches including hot gas heating, infrared radiation, ultrasonic and electric resistive heating [24]), there will always be a disadvantage of production speed compared to roller methods. However, maintaining a good replication quality especially with regard to large aspect ratios is the crucial challenge for roller embossing and related processes.

In the variothermal extrusion embossing process multiple advantages of the variothermal hot embossing and roller embossing are combined and enhanced by the advantages of the extrusion process. Instead of the two-step roller embossing process where a polymer film is extruded first and afterwards reheated and structured in a second step, the extrusion embossing combines both methods into one single production technique [23]. Thus, unnecessary handling of material is avoided. It also allows for less exposure of the polymer to high temperatures and higher overall production rates as the time, energy and equipment for the reheating step can be saved. Compared to the standard extrusion process the polished chill roll of the calender is replaced by a micro-structured embossing roll. This roll has the negative structure of the latter film surface (e.g. holes in the roll will result in elevations on the film). The embossing roll which functions as a master for replication can be produced with any suited manufacturing method (e.g. laser ablation or micro machining). Furthermore, in order to improve and adjust the fidelity of replication a variothermal heating system is added to the process [21,22,25]. This system generates a temperature profile along the circumference of the liquid cooled embossing roll. Hence, not only the production speed can be increased as the viscosity of the polymer is lower in the embossing zone but also the quality of the replication is greatly improved [23,25]. Besides the above mentioned methods for variothermal heating a laser- or an inductor-based system can deal with the high specific output power required for this task.

This paper covers some basic principles of the variothermal extrusion embossing process applying a laser-based heating system. The reproduction of super hydrophobic, lotus leaf-like structures is investigated and an analysis of the replication fidelity and the static contact angle is presented. Contact angle hysteresis and theoretical approaches beyond the classical Wenzel [26] and Cassie-Baxter [27] models are not within the scope of this work. This paper focuses on the influence of the heating power of the variothermal heating device as well as on the basic temperature of the embossing roll with respect to surface structure, replication fidelity and contact angle.

2 EXPERIMENTAL DETAILS

2.1 Variothermal extrusion embossing

This paper focuses on the results obtained by applying variothermal extrusion embossing. Figure 2 shows the underlying concepts and schematic set-up of the process. In the following the fundamentals are briefly summarised. Further details are found in work recently published [21,22-25].

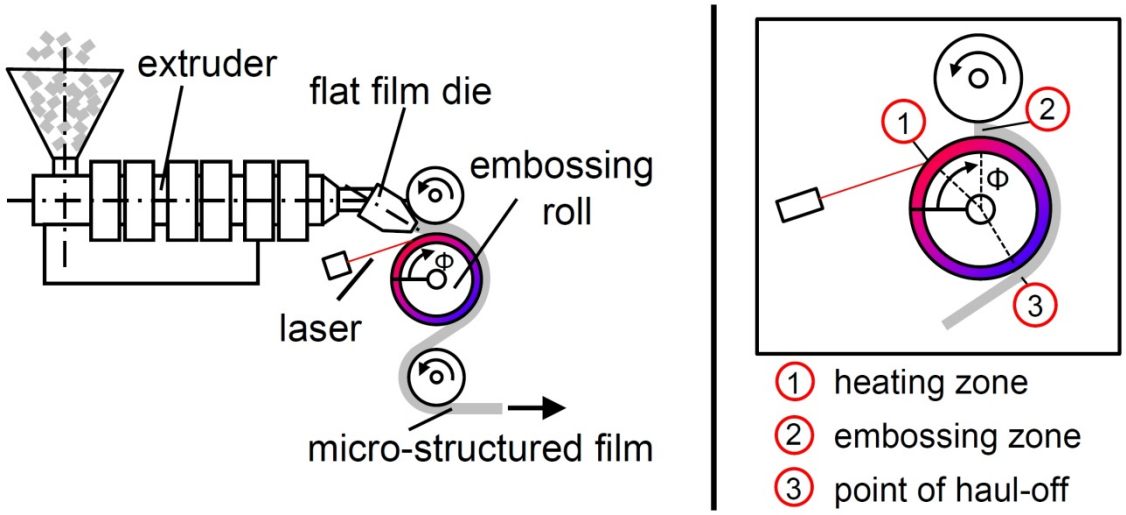

Figure 2: Schematic set-up of the variothermal extrusion embossing process
left: schematic set-up of variothermal extrusion embossing process
right: enlargement of the embossing roll

In extrusion embossing a polymer melt is delivered by the extruder and shaped by the flat film die. The melt temperature is controlled and can be adjusted by the extrusion process. The melt touches the embossing roll of the calender right in front of the embossing zone and is embossed. The line force applied by the weight of the counter pressure roll is the driving force in the replication process.

Governing process parameters are melt temperature, viscosity, surface temperature of the embossing roll and rotation speed of the roll. At the point of haul-off the polymer film is removed from the embossing roll. In addition to the peel-off angle and the rotation speed of the roll, the temperature of the polymer film and hence the material behaviour is of great importance when demoulding the surface structures.

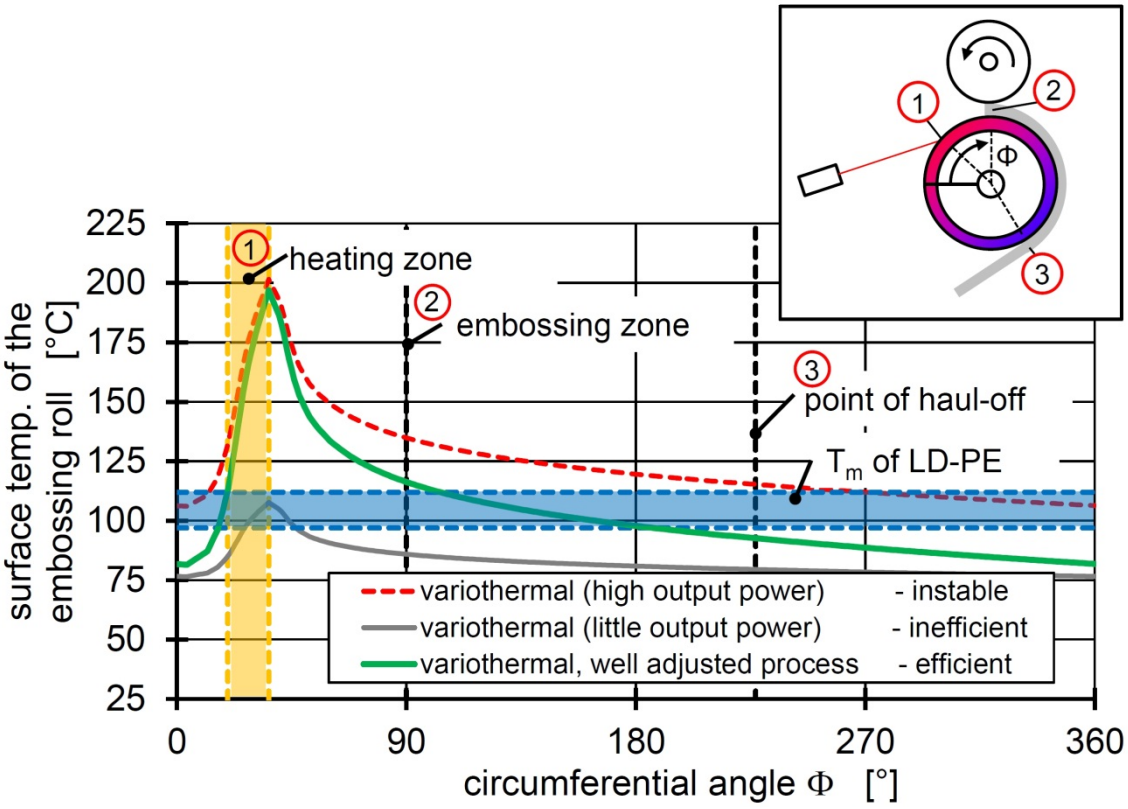

Figure 3: Potential temperature profiles along the circumference of the embossing roll's surface

Consequently, the temperature profile along the circumference of the embossing roll is of great interest for the replication of microstructures. Figure 3 shows possible temperature profiles along the circumference of the embossing roll's surface. It is expected that changing the profile will distinctively influence the fidelity of replication. As generally accepted, good replication requires temperatures of the melt and the roll in the embossing zone higher than the melting temperature T_m of the polymer [19,23,28]. The temperature profile along the circumference is influenced by many parameters. Haul-off speed, output power of the laser and basic temperature of the embossing roll are the most dominant ones. As illustrated in Figure 3 the embossing zone in extrusion embossing is due to construction conditions not exactly at the position of the temperature peak but close to it. It is desirable to keep this distance as low as possible since the gradient of the temperature profile is most pronounced in this area. Consequently, for the replication process only the total temperature

difference between the embossing zone, where the temperature should be above T_m, and the haul-off point, where sufficient low temperatures are required for a stable haul-off of the polymer film, is of interest. Achieving this temperature profile is challenging and usually requires very slow haul-off speeds, high output powers and an actively cooled embossing roll. This combination is usually not feasible so that embossing in extrusion embossing, contrary to hot embossing, takes places even at surface temperatures of the embossing roll below T_m.

The embossing roll used for the experiments presented in this paper was produced using pico-second (ps) laser ablation. The surface is subsequently coated with $(Cr_{0.73}Al_{0.27})N$ using physical vapour deposition (PVD) to protect the structures implemented in the embossing roll and decrease the release forces. The micro-structure chosen for this study is a replica of the lotus structure as described by Barthlott et al [5]. Figure 4 shows the original structure of a lotus leaf as reported in literature, the master surface of the embossing roll as produced by laser ablation with additional PVD coating and an example of the replicated surface structure obtained after processing a low density polyethylene (LD-PE). In this paper samples from different process settings are compared with respect to the surface structure, the replication fidelity and the functionality of the surface in terms of the static contact angle of purified water.

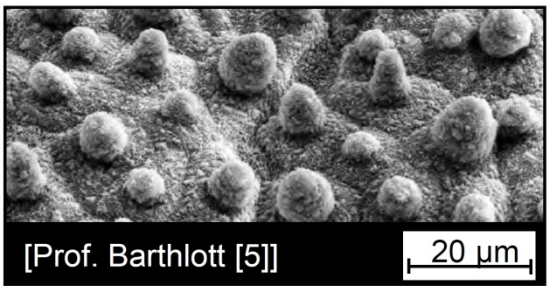

real geometry:
aspect ratio: 0.67 – 10
cone-like, unregularly spaced structures
height: 10 – 50 µm
base diameter: 5 – 15 µm
spacing: 10 – 100 µm

static contact angle: 156° – 161°

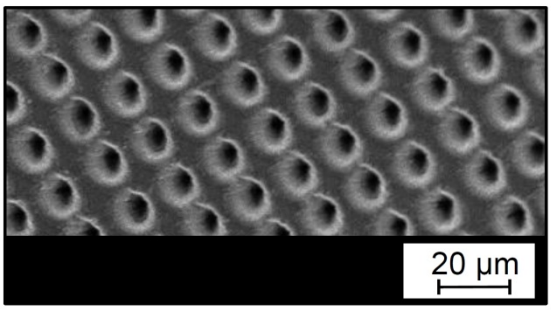

master surface of the embossing roll:
regular holes
depth: appr. 15 µm
base diameter: 10 µm
spacing: 5-10 µm

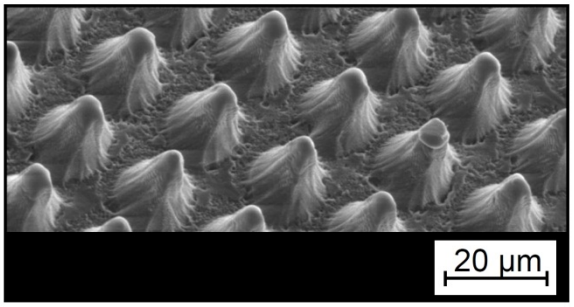

artificial geometry:
aspect ratio: 1.2
regular cones
height: 12 µm
base diameter: 10 µm
spacing: 5 – 10 µm

Figure 4: Mimicking nature – lotus leaf, master tool for replication and replica

top: natural lotus leaf [5]
bottom left: surface structure of the embossing roll
bottom right: replicated microstructure of a PP film

The manufacturing process of the embossing roller is summarised in the following.

2.2 Laser ablation – structuring of the embossing roll

The requested micro structure for the finished embossing roll is a hole structure with a hole diameter of 10 µm and a depth of 15 µm. The production of the embossing roll includes a laser structuring process followed by a coating process. As the holes will be scaled down due to the coating process the micro structures have to have a geometry of 12 µm diameter and approximately 16 µm depth after laser structuring.

Therefore the laser structuring experiments are carried out with a diode pumped Nd:YVO_4 MOPA laser (Master Oscillator Power Amplifier; Rapid, LumeraLaser) at a wavelength of λ = 355 nm. The laser operates at repetition rates up to ν = 500 kHz and a pulse duration of τ = 12 ps. Due to the ultra-short laser pulses the laser structuring is vapour dominated instead of melt dominated. This leads to a more homogeneous structuring of small structures [29,30]. The wave

length is chosen as small holes have to be generated on a large area. Due to the short wave length a longer focus length can be used and therefore a scanner lens with larger scan field.

For the micro structuring experiments the laser focus is positioned on the surface of the embossing roll by a galvanometer scanner system (intelliSCAN-14-DE, Scanlab) with a focus length of f = 56 mm (focus diameter ca. 12 µm). As the hole area cannot be structured within one scan field, several scan fields have to be positioned next to each other. To blur the edges of the scan fields an adapted strategy has to be applied.

The holes are generated in a percussion drilling process. Each hole is drilled with several pulses with still standing laser beam. For adaption of the diameter the pulse energy is varied. For adaption of the depth the number of pulses is varied. The distance of the holes is minimised. The presented holes are drilled with the parameters in Table 1.

repetition rate	output power	number of pulses	distance of the holes
400 kHz	50 mW	1200	15 µm

Table 1: Parameters for laser drilling process

The analysis of the master structure of the micro-structured roll is a challenging task. Since the sleeve of the structured embossing roll has a diameter of 144 mm, a roll face width of 350 mm and a weight of approximately 33 kg, it usually does not fit inside common scanning electron microscope (SEM) chambers or onto specimen tables of other microscopy systems. Therefore, images are obtained at the Central Facility of Electron Microscopy at RWTH Aachen University using a Large-Chamber SEM (LC-SEM). The size and weight limitations imposed by the geometry of the chamber and the goniometer can pose severe problems in standard scanning electron microscopes. In the LC-SEM the column itself is suspended and can move around the object. The object can thus have dimensions of up to 70 cm in diameter and 300 kg in weight. In the microscope a combination of analytical capabilities consisting of the standard SE, BSE detectors and a liquid nitrogen free EDX detector is available.

2.3 PVD coating for the embossing roll

The structures which are generated by laser structuring increase the surface area of the tool. This favours the effect of adhesion of the moulding material to the tool, which can affect the demoulding of the component negatively. The small structures are also exposed to considerable wear from abrasion and

adhesion. In order to address these challenges, it is necessary to develop hard material coatings which reduce not only the adhesion of the moulding mass but also the wear of the moulding tool. The magnetron sputter ion plating (MSIP) PVD technology has been applied for the deposition of the coating. The coating unit CC800/9 SinOx by CemeCon AG, Würselen, Germany, is equipped with power supplies using bipolar pulsed middle frequency (MF) pulses for sputtering. To get the aimed chemical composition Cr targets with 20 pieces of diameter 15 mm Al plugs (CrAl20) (purity: Cr 99.9 % and Al 99.5 %) and Al targets with 20 pieces of diameter 15 mm Cr plugs (AlCr20) (purity: Al: 99.5 % and Cr: 99.9 %) are used. The deposition parameters are listed in Table 2. On the one side the embossing roll made of 42Cr13 (AISI 420) and 42Cr13 specimens were coated within this batch. On the other side specimens made of cemented carbide were coated for some analyses.

Process parameter	**Unit**	**Value**
Substrate		42Cr13 (AISI 420) / Cemented Carbide
Targets		CrAl20/AlCr20
Time t	min	55
Temperature T at heater	°C	570
Argon flow F(Ar)	sccm	120
Krypton flow F(Kr)	sccm	80
Nitrogen flow F(N_2)	sccm	105
Pressure p	mPa	570
Bias voltage U_{Bias}	V	-120
Cathode mean power $\overline{P}$	kW	2 x 6.0
Frequency f	kHz	18.51
Pulse duration τ	ns	7

Table 2: Deposition parameters of the used coating system

In order to evaluate the morphology and the thickness, scanning electron microscope (SEM) micrographs of fractured cross sections were taken (ZEISS DSM 982 Gemini) using SE (secondary electrons) mode. Within this SEM an energy dispersive X-ray spectroscopy (EDS) was used to determine the chemical composition of the surfaces. Hardness and Young's modulus were, moreover, determined using the method of nano indentation. A Nanoindenter XP by MTS Nano Instruments was applied for this purpose. The indentation depth did not exceed 1/10 of coating thickness. The evaluation of the measured results was based on the equations according to Oliver and Pharr [31]. A

constant Poisson's ratio of v = 0.25 was assumed. Roughness of the coating was measured by means of 3D laser scanning microscopy (Keyence VK-9710).

Fehler! Verweisquelle konnte nicht gefunden werden. shows on the left a SEM cross section fracture of the $(Cr_{0.73}Al_{0.27})N$ coating. It shows a dense and fine grained morphology. Also a smooth surface structure is visible. The morphology as well as the surface structures lead to the assumption that this coating has a high hardness, a low roughness and a high corrosion resistance against common reactions in plastics melt. On the right of **Fehler! Verweisquelle konnte nicht gefunden werden.** a SEM image of the coated embossing roll is shown.

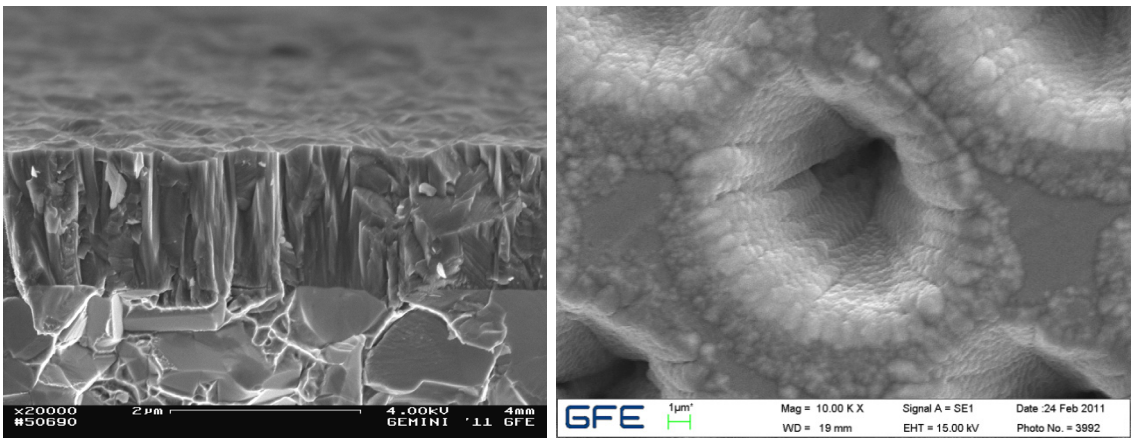

Figure 5: SEM cross section fracture micrograph of $(Cr_{0.73}Al_{0.27})N$ on cemented carbide (left) and SEM of the coated, micro structured embossing roll (right)

The achieved coating properties are listed in Table 3. The coating has a high hardness of about 26.1 ± 3.5 GPa and a Young's modulus of 453 ± 55 GPa. This leads to the assumption that a good protection of the structures against abrasive wear can be reached. Furthermore, the surfaces of the coating show a low roughness of Ra 0.059 µm.

Coating properties	Unit	Value
Chemical composition		$(Cr_{0.73}Al_{0.27})N$
Thickness d	µm	1.5
Deposition rate R	µm/h	1.6
Hardness H	GPa	26.1 ± 3.5
Young's modulus E	GPa	453 ± 55
Arithmetic average roughness Ra	µm	0.059
Root mean squared roughness Rq	µm	0.079

Table 3: Properties of the deposited coating

2.4 Experimental design

Experiments are performed processing low density polyethylene (LD-PE), Lupolen 2420 K, Basell Polyolefine GmbH, Wesseling, Germany, at a processing temperature of 190 °C. For the experiments the net output power of the laser heating system is subsequently increased in steps of 325 W starting at 0 W. Experiments performed with an output power of 0 W correspond to a conventional roller embossing process. The maximum output power feasible is 1625 W. Beyond this point no stable process can be achieved due to lacking solidification of the polymer melt. The speed of the embossing roll is kept constant at 1 m/min. The basic temperature of the water cooled embossing roll is changed between 50 °C and 70 °C respectively.

For the performed experiments a laboratory scale extruder, Collin 3250 25 90, and a chill-roll calender, Collin CR 136 / 350, both Dr. Collin GmbH, Ebersberg, Germany, equipped with an embossing roll are used. The surface structure of the embossing roll (the master surface) is created by applying pico-second laser ablation techniques at the Fraunhofer Institute of Laser Technology, see chapter 2.2. Holes with the negative shape of truncated cones are obtained with an average base diameter of 10 µm and depth of 15 µm. The used coathanger die has an outlet geometry of 155 mm outlet gap width and 500 µm gap height. All characteristic parameters of the set-up are summarized in Table 4. The thickness of the produced films is held constant at 538 ± 23 µm in order to have comparable conditions and pressure distributions in the embossing zone. Only a small band of 15 mm is structured on the embossing roll.

external heating device	
diode laser system, LDF 1500-2700, Laserline GmbH	max. output power = 2.7 kW wavelength = 940 nm and 980 nm heating zone: length = 10 mm width = 68 mm distance between optic and roll surface = 300 mm angle of irradiation = 18°
laboratory scale extruder	
laboratory scale extruder type 3250 25 90, Dr. Collin GmbH	screw diameter = 25 mm screw length = 25 D
embossing calender	
Collin CR 136 / 350, Dr. Collin GmbH	haul-off speed used = 1 m/min
embossing roll	
negative master for the replication process	outer roll diameter = 144 mm micro structure geometry: base diameter = 10 µm hole depth = 15 µm aspect ratio = 1.5 distance between holes = ca. 3 µm

Table 4: Characteristic set-up parameters

2.5 Evaluation of obtained samples

Film samples are analysed using a scanning electron microscope (SEM), Zeiss DSM 960 A, Carl Zeiss AG, Oberkochen, Germany. Furthermore, confocal laser microscopy VK-9710, Keyence Deutschland GmbH, Neu-Isenburg, Germany, is employed to measure the average geometry of the analysed samples. Results presented in the following are average values out of five measurements.

Sessile drop contact angle measurements against distilled water are performed by means of a OCA 20, DataPhysics Instruments GmbH, Filderstadt, Germany. The volume of drops analysed is in the range of 9 µl ± 1 µl.

The process parameters “characteristic heating power of the laser heating system”, “haul-off speed” and “basic temperature of the water cooled embossing roll” are recorded and used for the calculation of the temperature profiles according to [21], [22] and [23]. The characteristic heating power $P'_{heat,Laser}$ is the effective output power of the laser system that is absorbed by the embossing roll along the circumference of the roll (Eq. 1). The total output power of the laser is therefore multiplied with the degree of efficiency and divided by the width of the heating zone.

$$P'_{heat,Laser} = \frac{P_{heat}}{width} \cdot \eta^*_{Laser} \qquad \text{Eq. 1}$$

The degree of efficiency η^*_{Laser} for the absorption of energy by the roll is estimated to $\eta^*_{Laser} = 0.451$ in good agreement with measurements [23].

3 RESULTS AND DISCUSSION

In the following, the produced surfaces are analysed in terms of their geometry and their functionality when applying static contact angle measurements with purified water.

Figure 6 gives an overview of SEM-images obtained from the produced surfaces. Samples are produced with haul-off speeds of 1.0 m/min. The cooling temperature of the embossing roll is set to either 50 °C or 70 °C and the output power of the external heating device is increased subsequently. The first image of each row shows the results of a conventional embossing process without using an external heating device for variothermal process control. It is evident that even without variothermal heating a shaping of the surface can be achieved. However, the fidelity of replication and geometry of the resulting structures are limited. Particularly, higher aspect ratios (ratio of height to base diameter of the structure) and small structures with dimensions in the micro range can hardly be replicated. Applying even modest variothermal temperature control, results are remarkably improved. As shown in Figure 6 the surface geometry slowly develops and the structures gain height. Another observation is the formation of hair-like structures at the tip of the replicated cones. This becomes even more evident when further increasing the output power of the variothermal heating device. This indicates that stretching and deformation take place due to reduced stiffness at higher temperatures.

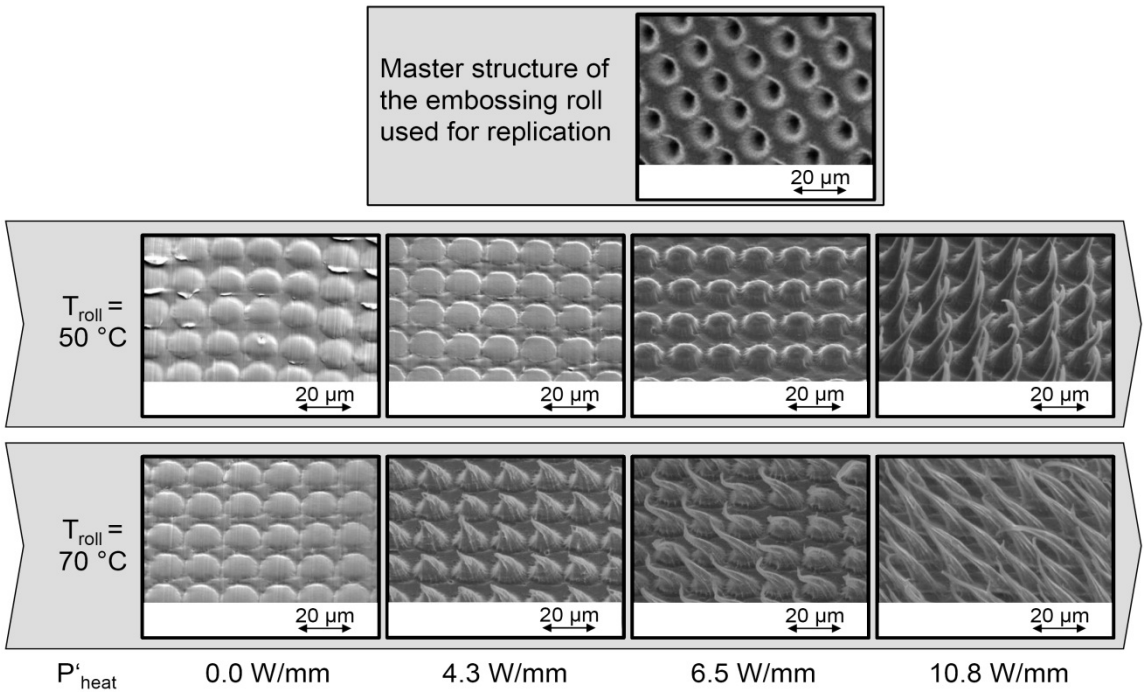

Figure 6: Overview of SEM-images of LD-PE film samples produced at different sets of process parameters

Though the reason for the formation of these “hairs” is yet not completely understood, it seems to be likely that undercuts of the master structure are filled by the plastics melt at high temperatures since the viscosity is reduced. After solidification this leads to locking. Hence, deformation as well as stretching is favoured at the haul-off point. A higher temperature level not only reduces the viscosity in the embossing zone, it also causes higher temperatures at the haul-off reducing the resistance against deformation.

3.1 Fidelity of replication

In order to further describe the geometry of the produced surface structures confocal laser microscopy (CLM) is employed. Figure 7 shows examples of CLM-images in comparison to SEM-images shown earlier. Applying confocal laser microscopy average values for the structure height are derived from each sample and analysed.

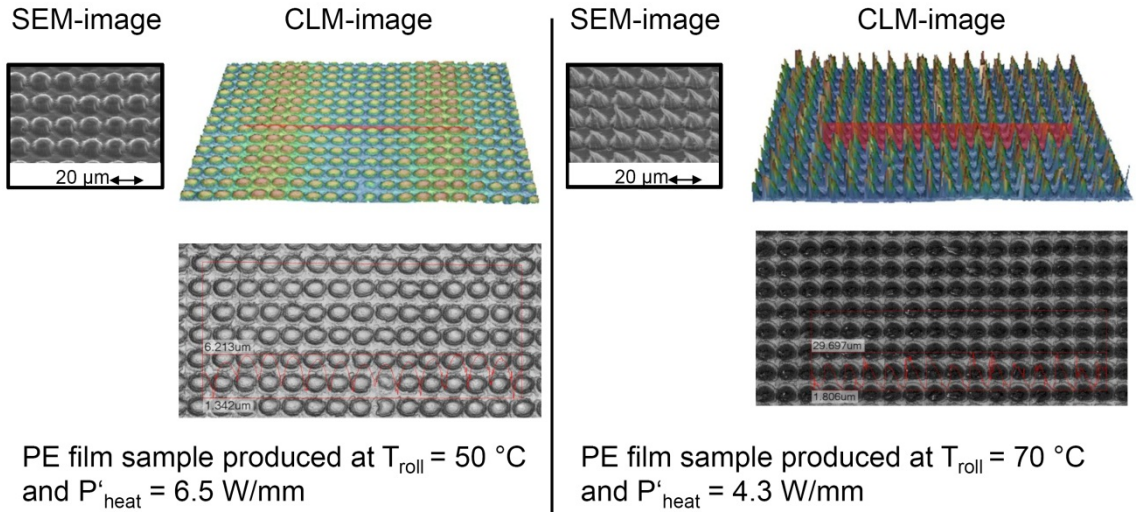

Figure 7: Examples of confocal laser microscopy (CLM) images

Figure 8 summarises the dependency of the produced structure heights on the characteristic heating power and the cooling temperature of the embossing roll. Starting with very small values for the structure height, this slowly changes until reaching a transition zone and finally ending in a high plateau. This clearly indicates the potential of the variothermal heating.

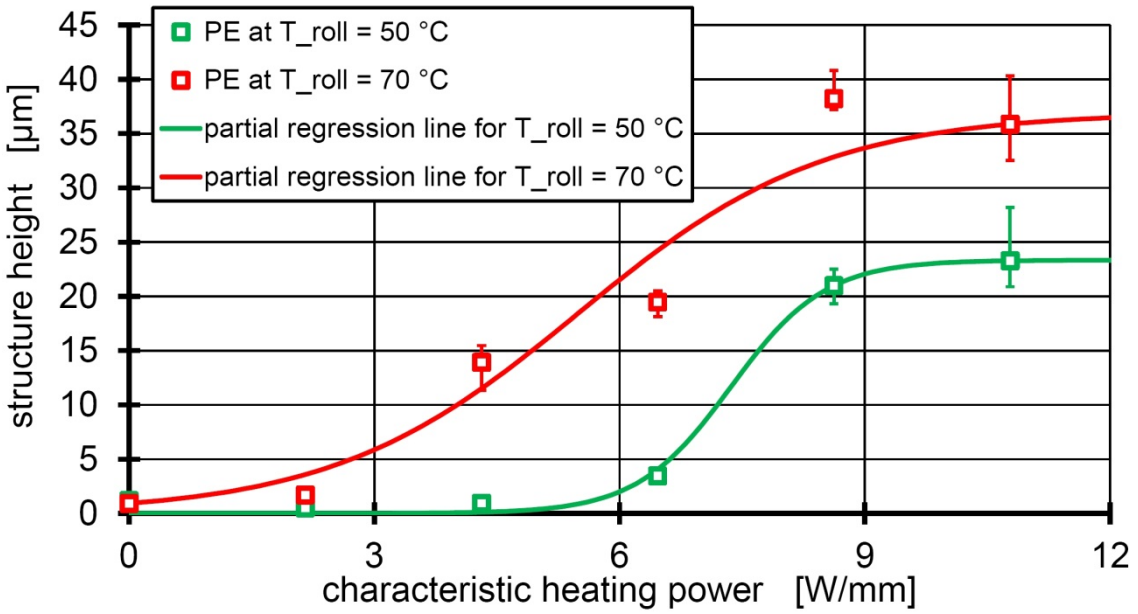

Figure 8: Influence of the characteristic heating power on the measured structure height for LD-PE film samples produced at 1.7 m/min and 50 °C as well as 70 °C water cooling temperature of the embossing roll, respectively

These observations are in good agreement to the SEM-images. It seems that with higher general temperature levels of the embossing roll (here at T_{roll} = 70 °C) the achievable structure heights are higher than at lower temperature levels. Taking the base diameter of 10 µm into account, structures with aspect ratios in the range of 3.5 to 4 can be produced; however, this is obviously not a 100 % replication of the master structure but a result of the pronounced deformation of the structures and the formation of hairs during haul-off.

As a transition from a lower plateau at low characteristic heating powers to another upper plateau at high powers is observed, a hyperbolic tangent formulation (Eq. 2) is chosen to mathematically describe the observed behaviour. Applying a least square fitting the parameters c_1, c_2 and c_3 are calculated and summarised in Table 5. c_1 represents the mean value of the two plateaus and c_2 the shift of the curve with respect to the characteristic heating power. c_3 is the scaling factor for the slope of the curve in the transition from the lower to the upper plateau. The equation describes the dependency between the resulting structure height and the characteristic heating power.

$$structure\ \ height = c_1 \cdot \left(1 + \tanh\left[\left(P'_{heat} + c_2\right) \cdot c_3\right]\right) \qquad \text{Eq. 2}$$

Case	Cooling temperature of the embossing roll [°C]	Haul-off speed [m/min]	c_1 [µm]	c_2 [W/mm]	c_3 [mm/W]
1	50	1.0	11.671	-7.364	0.869
2	70	1.0	18.470	-5.500	0.334

Table 5: Constants c_1, c_2 and c_3 of the hyperbolic tangent equation for describing the structure height based on the characteristic heating power

Future work should focus on using this equation and deriving correlations between the constants c_1, c_2 and c_3 and process parameters like cooling temperature of the embossing roll and haul-off speed. Thus, a first rough prediction of the structure height seems possible.

A first application of this idea is described in the following equations Eq. 3, Eq. 4, Eq. 5 and the corresponding Table 6. A simple, linear correlation is assumed with terms for the haul-off speed and the surface temperature of the embossing roll. Thus, the parameters c_1, c_2 and c_3 can be calculated with respect to these

process parameters. However, the derivation and evaluation of these equations is not within the scope of this paper and should be understood as a motivation and outlook for further research. This will require a larger experimental design taking into account a variation of the haul-off speed as well as varying the cooling temperature of the embossing roll and changing the characteristic heating power. Hence, the author wants to stress that values given in Table 6 exactly match the findings of this specific example but would lead to wrong assumptions for other sets of processing parameters.

$$c_1 = c_{1,0} + c_{1,haul-off} \cdot v_{haul-off} + c_{1,roll} \cdot T_{roll} \quad \text{Eq. 3}$$

$$c_2 = c_{2,0} + c_{2,haul-off} \cdot v_{haul-off} + c_{2,roll} \cdot T_{roll} \quad \text{Eq. 4}$$

$$c_3 = c_{3,0} + c_{3,haul-off} \cdot v_{haul-off} + c_{3,roll} \cdot T_{roll} \quad \text{Eq. 5}$$

$c_{1,0}$ [µm]	$c_{1,haul-off}$ [µm · min/m]	$c_{1,roll}$ [µm · 1/K]	$C_{2,0}$ [W/mm]	$c_{2,haul-off}$ [W/mm · min/m]	$c_{2,roll}$ [W/mm · 1/K]	$C_{3,0}$ [mm/W]	$c_{3,haul-off}$ [mm/W · min/m]	$c_{3,roll}$ [mm/W · 1/K]
-99.18	1	0.334	-38.48	1	0.093	8.52	1	-0.027

Table 6: Constants for calculating c_1, c_2 and c_3

As the haul-off speed is not varied in the here presented work, the corresponding factors $c_{i,haul-off}$ are arbitrarily set to 1. The other factors $c_{1,0}$, $c_{1,roll}$, $c_{2,0}$, $c_{2,roll}$, $c_{3,0}$ and $c_{3,roll}$ are derived by solving the equations with respect to the process parameters used. For a prediction of the shape of extrusion embossed film surfaces, the influence of the master geometry as well as distinctive material characteristics of the processed polymer will have to be incorporated and are scope of future research.

After analysing the influence of the heating power on the obtained structure height, the functionality of the surfaces is determined in terms of static contact angle measurements against purified water.

3.2 Functionality in terms of static contact angles

Figure 9 depicts examples of water drops that are observed on the plastics film surface. It is evident that at higher characteristic heating powers P'_{heat} the observed changes of the surface texture result in stronger hydrophobic surface characteristics. The drops are shaped more spherically indicating increased static contact angles. Again, using a higher temperature level for the embossing roll strongly improves the functionality of the obtained surfaces as drops have higher contact angles at T_{roll} = 70 °C when comparing the same heating power.

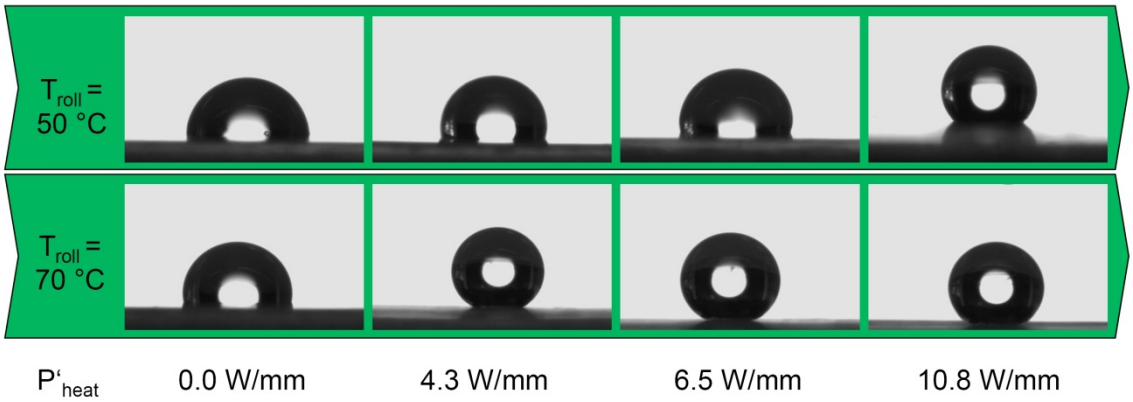

Figure 9: Examples of the resulting shapes of water drops on the produced LD-PE film samples – the samples are according to the SEM-samples of Figure 6

To quantitatively study the contact angles, measurements are summarised in Figure 10. Similar to the findings when analysing the structure height, the transition from one plateau at low heating power to an upper plateau for high heating powers is observed. It seems that it is hardly possible to exceed values above 150°. At least for the material used such values were not measured. Comparing the two lines in Figure 10, the graph for PE at 50 °C converges more slowly towards the upper threshold. Furthermore, the transition seems to be extended to a larger range allowing for a more precise adjustment if values in this range are required. However, if the interest is a maximum of the static contact angle higher cooling temperatures for the embossing roll lead to better results at the same heating power of the external heating device. In the presented experiments the static contact angle of LD-PE is improved up to 150° which is a gain of at least 50 % compared to unstructured (90° - 100°) or conventionally structured (around 100°) surfaces (see Figure 10). This clearly indicates the potential of using variothermal processing for extrusion embossing of micro structured films.

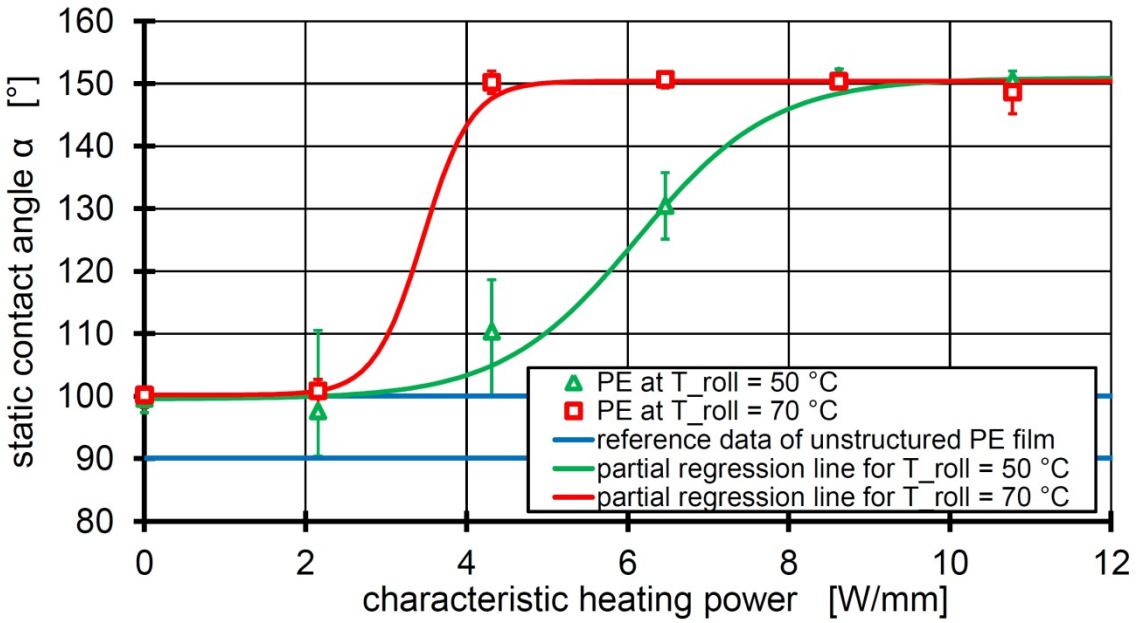

Figure 10: Correlation between the measured static contact angle against purified water and the characteristic heating power used for producing the surface structures in the variothermal extrusion embossing process

As already discussed in the section on the fidelity of replication, a comparable hyperbolic tangent formulation can be used to describe the static contact angle as a function of the characteristic heating power. The corresponding constants for Eq. 5 are listed in Table 7.

$$static\ \ contact\ \ angle = c_{1\alpha} \cdot \left(1 + \tanh\left[\left(P'_{heat} + c_{2\alpha}\right) \cdot c_{3\alpha}\right]\right) \qquad \text{Eq. 6}$$

Case	Cooling temperature of the embossing roll [°C]	Haul-off speed [m/min]	$c_{1\alpha}$ [°]	$c_{2\alpha}$ [W/mm]	$c_{3\alpha}$ [mm/W]
1	50	1.0	25.678	-6.119	0.595
2	70	1.0	25.105	-3.456	1.656

Table 7: Constants $c_{1\alpha}$, $c_{2\alpha}$ and $c_{3\alpha}$ of the hyperbolic tangent equation for describing the static contact angle based on the characteristic heating power

3.3 Studying the temperature profiles along the roll's circumference

Studying the surface temperature of the embossing roll as a result of the process parameters used allows for better understanding of the various surface structures that are generated. Figure 11 gives an overview of some of the calculated temperature curves. These curves are obtained performing finite element analysis on the surface temperature by varying the process parameters in a wide range [23]. Considering these observations it is possible to derive a standardised master curve as well as equations that describe the surface temperature in terms of the chosen process parameters. The relevant theory is described in literature in more detail (e.g. see [23]) and is only applied in this paper to obtain an estimation of the resulting surface temperature of the embossing roll with regard to the chosen process settings.

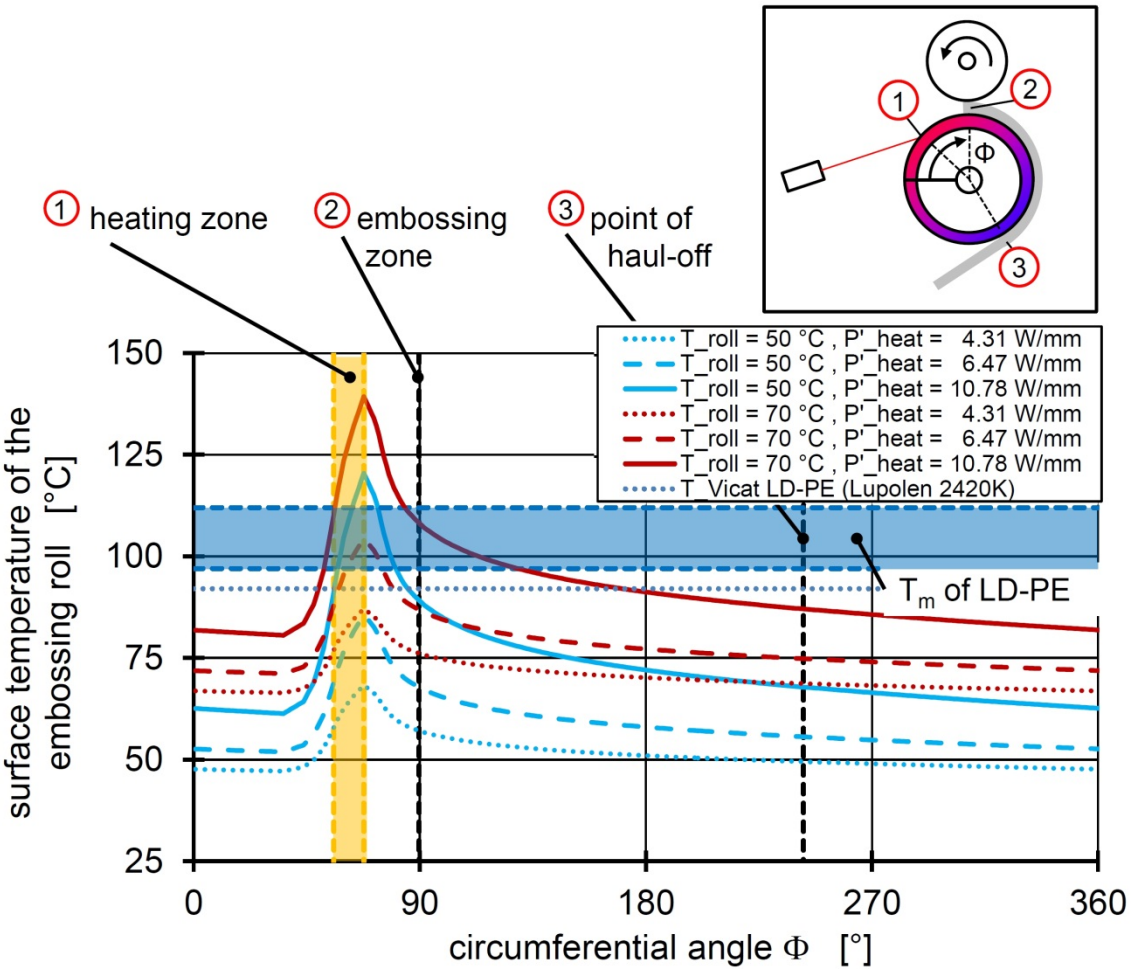

Figure 11: Temperature curves calculated for different sets of basic temperature of the embossing roll and characteristic heating power

As can be seen in Figure 11, the overall temperature level greatly depends on the basic temperature of the embossing roll whereas the characteristic heating power is responsible for the shape of the temperature peak that is generated along the circumference of the roll. It is remarkable that almost all of the analysed sets of process parameters lead to temperatures in the embossing zone that are below the melting range of the LD-PE. They are also lower than the Vicat temperature T_{Vicat} that is 92 °C for the LD-PE studied. The Vicat temperature is used as the heat deflection temperature in this analysis. Table 8 gives a complete overview of the calculated temperatures at characteristic positions of the embossing roll. Only for T_{roll} = 70 °C in combination with P'_{heat} = 10.78 W/mm temperatures in the melting range are achieved. However, this does not seem necessary for achieving good fidelities of replication or good functionality. As discussed above, even other sets of process parameters that result in lower temperatures in the heating zone will give comparable results for both fidelity and functionality.

Comparing the SEM-images of Figure 6, it is obvious that those of T_{roll} = 50 °C and P'_{heat} = 10.78 W/mm and those of T_{roll} = 70 °C and P'_{heat} = 6.47 W/mm show similar surface pattern. Furthermore, both structures show comparable static contact angles. Looking at the temperature curves, these two curves result in comparable conditions in the embossing zone. However, the temperature at haul-off is different. Hence, the process conditions in the embossing zone seem to be more relevant for the surface structure than those during haul-off. Nevertheless, it should be stressed that the temperature at haul-off is very likely to be responsible for stretching and deformation if it exceeds or gets close to the heat deflection temperature of the material.

process parameters			characteristic temperatures			measurements	
characteristic heating power [W/mm]	cooling temp. of the embossing roll [°C]	haul-off speed [m/min]	maximum temp. at the end of the heating zone [°C]	temp. in the embossing zone [°C]	temp. at the haul-off point [°C]	average structure height [µm]	static contact angle [°]
0.00	50	1.0	38	38	38	1.2	100
2.16	50	1.0	51	46	43	0.5	98
4.31	50	1.0	68	57	49	0.9	110
6.47	50	1.0	86	68	56	3.5	130
8.62	50	1.0	103	78	62	21.0	151
10.78	50	1.0	120	89	68	23.3	151
0.00	70	1.0	57	57	57	0.9	100
2.16	70	1.0	70	65	63	1.7	101
4.31	70	1.0	87	76	69	13.9	150
6.47	70	1.0	105	87	75	19.5	151
8.62	70	1.0	122	98	81	39.2	150
10.78	70	1.0	139	108	87	35.9	149
characteristic temp. of LD-PE (Lupolen 2420 K)							
T_m = 97 °C – 112 °C			T_{Vicat} = 92 °C				

Table 8: Calculated temperatures according to [23] at characteristic positions of the embossing roll

4 CONCLUSIONS

The variothermal extrusion embossing process is suitable for manufacturing micro structured polymer films. In this paper the phenomena occurring when processing LD-PE are described and analysed. Cone-like surface structures comparable to those found on the leaves of a lotus are replicated in order to produce hydrophobic polymer films. The embossing roll is produced by means of laser ablation und afterwards coated with an $(Cr_{0.73}Al_{0.27})N$ coating in an PVD-process. Scanning electron microscopy, confocal laser microscopy and static contact angle measurements against purified water are applied to characterise and study the obtained film samples. The final demoulded surface structure can not only show a close to 100 % replication of the negative master structure of the embossing roll but also bad replications as well as strong deformation due to stretching during demoulding. Thus, hair-like structures with aspect ratios up to 4 and outstanding functionality are obtained.

How the temperature profile along the circumference of the embossing roll surface is shaped greatly depends on the process settings. The resulting microstructure depends on this temperature profile (the temperatures in the embossing zone and at the haul-off point) as well as on the material characteristics of the processed material, e.g. melting range, viscosity and heat deflection temperature. Using this knowledge, it is possible to adjust the surface geometry to specific requirements by changing the process settings.

Furthermore, the results presented above contribute to a better understanding of the process in general and support the prediction of extrusion embossing results. With respect to the functionality of the surface structures it is evident that hair-like structures show superior behaviour in terms of static contact angle measurements. Contact angles up to 150° are achieved. The structure height as well as the contact angle follow a hyperbolic tangent description, rising from a lower plateau through a transition zone up to an upper plateau while changing the characteristic heating power.

ACKNOWLEDGEMENT

The presented research has been funded by the German Research Foundation, Deutschen Forschungsgemeinschaft (DFG), as part of the program Cluster of Excellence “Integrative Production Technology for High-wage Countries”. The authors would like to thank DFG for the support. Furthermore, we thank Basell Polyolefine GmbH, Wesseling, for the donation of material.

REFERENCES

[1] Dean, B.; Bhushan, B. — Shark-skin surfaces for fluid-drag reduction in turbulent flow: a review. Philosophical Transactions of the Royal Society A 368 (2010) 1929, pp. 4775-4806

[2] Autumn, K.; Llang, Y.A.; Hsleh, S.T.; et al. — Adhesive force of a single gecko foot-hair. Nature 405 (2000) 6787, pp. 681-685

[3] Autumn, K.; Peattie, A.M. — Mechanisms of Adhesion in Geckos. Integrative and Comparative Biology 442 (2002) 6, pp. 1081-1090

[4] Clapham, P.B.; Hutley, M.C. — Reduction of Lens Reflexion by the "Moth Eye" Principle. Nature 244 (1973) 3, pp. 2881-282

[5] Barthlott, W.; Neinhuis, C. — Purity of the sacred lotus, or escape from contamination in biological surfaces. Planta 202 (1997), pp. 1-8

[6] Fürstner, R.; Barthlott, W.; Neinhuis, C.; Walzel, P. — Wetting and Self-Cleaning Properties of Artificial Superhydrophobic Surfaces. Langmuir 21 (2005) 3, pp. 956-961

[7] Heckele, M.; Schomburg, W.K. — Review on micro molding of thermoplastic polymers. Journal of Micromechanics and Microengineering 14 (2004), pp. R1-R14

[8] Krieger, K. — Do Pool Sharks Swim Faster. *Science* 305 (2004), pp. 636-637

[9] Giboz, J.; Copponnex, T.; Mélé, P.
Microinjection molding of thermoplastic polymers: a review
Journal of Micromechanics and Microengineering 17 (2007), pp. R96-R109

[10] Jiang, L.; Zhao, Y.; Zhai, J.
A Lotus-Leaf-like Superhydrophobic Surface: A Porous Microsphere/Nanofiber Composite Film Prepared by Electrohydrodynamics
Angewandte Chemie 116 (2004) 33, pp. 4438-4441

[11] Lau, K.K.S.; Bico, J.; Teo, K.B.K.; et al.
Superhydrophobic Carbon Nanotube Forests
Nano Letters 3 (2003) 12, pp. 1701-1705

[12] Shirtcliffe, N.J.; McHale, G.; Newton, M.I.; et al.
Porous materials show superhydrophobic to superhydrophilic switching
Chemical Communications 41 (2005) 25, pp. 3135-3138

[13] Yabu, H.; Shimomura, M.
Single-Step Fabrication of Transparent Superhydrophobic Porous Polymer Films
Journal of the American Chemical Society 127 (2005) 17, pp. 5231-5234

[14] Nie, Z.; Kumacheva, E.
Patterning surfaces with functional polymers
Nature Materials 7 (2008), pp. 277-290

[15] Groenendijk, M.
Fabrication of Super Hydrophobic Surfaces by fs Laser Pulses
Macro Material Processing 3 (2008), pp. 44-47

[16] Becker, H.; Heim, U. — Hot embossing as a method for the fabrication of polymer high aspect ratio structures. Sensors and Actuators A 83 (2000), pp. 130-135

[17] Gale, M.T. — Replicated Diffractive Optics and Micro-Optics. Optics & Photonics News 14 (2003) 8, pp. 24-29

[18] Chang, C.Y.; Yang, S.Y. Sheh, J.L. — A roller embossing process for rapid fabrication of microlens arrays on glass substrates. Microsystem Technologies 12 (2006), pp. 754-759

[19] Ng, S.H.; Wang, Z.F. — Hot roller embossing for microfluidics: process and challenges. Microsystem Technologies 15 (2009), pp. 1149-1156

[20] Bartolini, R.; Hannan, W.; Karlsons, D.; Lurie, M. — Embossed Hologram Motion Pictures for Television Playback. Applied Optics 9 (1970), pp. 2283-2290

[21] Michaeli, W.; Hopmann, C.; Eilbracht, S.; et al. — Manufacturing of micro-structured parts for mass production purposes. In: Conference Proceedings, International Symposium on Assembly and Manufacturing ISAM 2011, Tampere, Finland, (2011) 978-1-612884-343-8/11

[22] Michaeli, W.; Hopmann, C.; Kremer, C.; et al.
Variothermal Extrusion Embossing for Manufacturing of Micro-Structured Films
In: Conference Proceedings, 27th World Congress of the Polymer Processing Society PPS-27 2011, Marrakesh, Morocco, (2011) P-4-256

[23] Scharf, M.
Extrusionsprägen mikrostrukturierter Kunststofffolien
Dissertation (PhD-thesis), RWTH Aachen University, 2011

[24] Kimerling, T.E.; Liu, W.; Kim, B.H.; Yao, D.
Rapid hot embossing of polymer microfeatures
Microsystem Technologies 12 (2006), pp. 730-735

[25] Brecher, C.
Integrative Production Technology for High-Wage Countries
Springer, Berlin Heidelberg 2011

[26] Wenzel, R.N.
Resistance of solid surfaces to wetting by water
Industrial and Engineering Chemistry 28 (1936) 8, pp. 988-994

[27] Cassie, A.B.D.; Baxter, S.
Wettability of porous surfaces
Transactions of the Faraday Society 40 (1944), pp. 546-551

[28] Cameron, N.S.; Roberge, H.; Veres, T.; et al..
High fidelity, high yield production of microfluidic devices by hot embossing lithography: rheology and stiction
Lab on a Chip 6 (2006), pp. 936-941

[29]	Chichkov, B.N.; Momma, C.; Nolte, S.;von et al.	Femtosecond, picosecond and nanosecond laser ablation of solids Applied Physics A 63 (1996), pp. 109-115
[30]	Nolte, S.; Momma, C.; Jacobs, H.; Tünnermann, A.	Ablation of metals by ultrashort laser pulses Journal of the Optical Society of America B 14 (1997) 10, pp. 2716-2722
[31]	Oliver, W.C; Pharr, G.M.	An improved technique for determining hardness and elastic modulus using load and displacement sensing indentation experiments Journal of Materials Research 7 (1992) 6, pp. 1564-158

Keywords:
extrusion embossing, variothermal, super hydrophobic, contact angle, replication fidelity, micro structure, lotus leaf

Stichworte:
Extrusionsprägen, variotherm, superhydrophob, Kontaktwinkel, Abformgüte, Mikrostruktur, Lotusblatt

Author/Autor:
Dipl.-Ing. Stephan Eilbracht (Author)
Prof. Dr.-Ing. Christian Hopmann (Professor)
Prof. Dr.-Ing. Dr.-Ing. E. h. Walter Michaeli (Professor)
Institute of Plastics Processing (IKV)
RWTH Aachen University
Seffenter Weg 201
52074 Aachen
Germany

E-Mail-Adresse:
eilbracht@ikv.rwth-aachen.de
zentrale@ikv.rwth-aachen.de
Website: www.ikv-aachen.de
Phone.: +49(0)241/80-27271
Fax: +49(0)241/80-22316

Editor/Herausgeber:
Europe/Europa
Prof. Dr.-Ing. Dr. h.c. G. W. Ehrenstein, verantwortlich
Lehrstuhl für Kunststofftechnik
Universität Erlangen-Nürnberg
Am Weichselgarten 9
91058 Erlangen
Deutschland
Phone: +49/(0)9131/85 - 29703
Fax.: +49/(0)9131/85 - 29709
E-Mail: ehrenstein@lkt.uni-erlangen.de

The Americas/Amerikas
Prof. Dr. Tim A. Osswald,
responsible
Polymer Engineering Center,
Director
University of Wisconsin-Madison
1513 University Avenue
Madison, WI 53706
USA
Phone: +1/608 263 9538
Fax.: +1/608 265 2316
E-Mail: osswald@engr.wisc.edu

Publisher/Verlag:
Carl-Hanser-Verlag
Jürgen Harth
Ltg. Online-Services & E-Commerce,
Fachbuchanzeigen und Elektronische Lizenzen
Kolbergerstrasse 22
81679 Muenchen
Phone.: 089/99 830 - 300
Fax: 089/99 830 - 156
E-mail: harth@hanser.de

Editorial Board/Beirat:
Professoren des Wissenschaftlichen
Arbeitskreises Kunststofftechnik/
Professors of the Scientific Alliance
of Polymer Technology